

INTERNATIONAL SOCIETY FOR SOIL MECHANICS AND GEOTECHNICAL ENGINEERING



This paper was downloaded from the Online Library of the International Society for Soil Mechanics and Geotechnical Engineering (ISSMGE). The library is available here:

<https://www.issmge.org/publications/online-library>

This is an open-access database that archives thousands of papers published under the Auspices of the ISSMGE and maintained by the Innovation and Development Committee of ISSMGE.

Lessons Learned From Field Instrumentation and Remote Sensing Studies of Instrumented Pavement and Bridge Infrastructure

Anand J. Puppala¹, Ujwalkumar D. Patil² and Tejovikash Bheemasetti³

¹Distinguished University Professor, University of Texas at Arlington, anand@uta.edu

²Research Associate, University of Texas at Arlington, ujwalkumar.patil@uta.edu

³Research Associate, University of Texas at Arlington, tejovikash.bheemasetti@mavs.uta.edu

ABSTRACT

This keynote paper presents lessons learned from several field-based research studies conducted on pavement and bridge approach sites that were built on various treated materials, lightweight materials, and foundation systems. Field instrumentation, elevation surveys, and remote sensing studies, including terrestrial-based LiDAR studies, are described and analysed to give insight into the performance monitoring of these structures. Some of the data are compared with numerical analysis results to illustrate the benefits of using treated and lightweight materials to reduce pavement distress, such as rutting and differential cracking.

INTRODUCTION

Transportation infrastructure plays a prominent role in a nation's development, and over the years, several noteworthy innovations have taken place. These include new construction materials and procedures, and advanced methods of evaluating field performance. The most important evolutions pertain to the techniques employed to identify the distress patterns on pavements and bridge infrastructures.

Traditional surveying methods, such as robotic total station, tacheometry, 3D scanners, GPS, and others are labor intensive, costly, and very often time-consuming. However, under most conditions, particularly for a large area, a combination of remote sensing, using satellites and unmanned aerial vehicle systems (UAVs), and photogrammetric techniques has proven to be an inexpensive and viable alternative to conventional land surveying techniques (Mills and Newton, 1996; Ahmad, 2006; Uddin and Ahmad, 2014; Room and Ahmad, 2014; Siebert and Teizer, 2014).

Remote sensing techniques, such as synthetic aperture radar (SAR), interferometric synthetic aperture radar (InSAR), Johnson satellite differential interferometry (DInSAR), satellite thermal imagery, light detection and ranging (LIDAR), and unmanned airborne vehicles (UAVs) are used to collect sophisticated data on various infrastructures (Tripolitsiotis et al., 2014; Oscar et al., 2013; Tronin, 2010; Rathje et al., 2006). This data can be analyzed to assess the performance of the civil infrastructure.

The utilization of UAVs is gaining momentum due to their role in civil missions, such as aerial photography, surveillance and control of maritime traffic, fishing and farming surveillance, detection and control of coastal hazards, flood monitoring, terrain mapping, fire disasters, reconnaissance surveys, remote data acquisition of existing pavement conditions, and earthquake damage assessment (Adu-Gyamfi et al., 2014; Shamsabadi et al., 2014; Oscar et al., 2013; Tahar and Ahmad, 2012; Pereira et al., 2009; Rathje et al., 2006).

The first section of this paper briefly introduces remote sensing technology, using an unmanned aerial vehicle system (UAV) and its application to monitor pavement and bridge infrastructures. The second section introduces various materials used in soil treatment, especially chemical treatments for ground improvement, and briefly discusses a case study related to the performance of geofoam material in embankments to reduce pavement distress. In addition, the field instrumentation implemented at this site and the data obtained from it are discussed. The following sections present the details of these studies.

UNMANNED AERIAL VEHICLE SYSTEMS (UAVs)

Rotor wing and fixed wing are the two types of UAV units. Studies suggest that the difference is small between the photogrammetric output obtained from a fixed platform and mobile platform, such as a light-weight rotary wing UAV; hence, the unmanned aircraft system (UAS) can be used for large-scale mapping of aerial terrain (Tahar and Ahmad, 2012).

Close Range Photogrammetry

UAVs have become a popular tool in the past decade due to their versatility. Photogrammetry, using UAVs, can provide a digital elevation model (DEM) and a good quality digital terrain model (DTM) in a short period. The main advantage of UAS technology over traditional surveying techniques is its capability to capture direct, rapid, and detailed images of the study area. The adoption of UAVs for photogrammetry comes under the category of close-range photogrammetry (CRP) (Siebert and Teizer, 2014; Colomina and Molina, 2014). In this paper, this technology is referred to as UAS-CRP.

The three main components of UAS and CRP are the unmanned aerial vehicle, the ground control station, and the communication data link. The system can be controlled from the ground control station (GCS). The availability of GPS and gyroscope technology allows the UAV to precisely deliver the digital camera to the best location and altitude to capture the environment. In photogrammetry, it is a common practice for the ground control point (GCP) to be established after the aerial photography session. There are several methods that can be used to establish the GCP, such as traversing and the Global Positioning System (GPS) (Cesetti et al. 2011).

Rotary and Fixed Wing Type UAV

Fig. 1 shows commercially-available rotary-type UAV (Aibotix X6 multi-rotor) and fixed wing (UX 5) type UAV, both of which are available from Leica Geosystems. Aibotix X6 is a versatile UAS, best suited for acquiring data over relatively small areas. The hovering capability of the aircraft provides a unique data collection platform that can be applied to many areas. The Aibotix X6 multi-rotor UAS can be adopted for small-scale investigations, and the UX5 fixed wing UAS can be adopted for large-scale environments. The Aibotix X6, with an on-board RTK GPS receiver, allows the UAS to communicate and use real-time kinematic positioning provided by the existing TxDOT VRS network.

Fixed wing aircraft systems are better suited for collecting data in remote areas far from roadways with limited access. UX5 is a high-performance system with 50 minutes of flight time per battery charge and a 50 mile per hour cruise speed. This allows rapid collection of data over large areas. At a 2-inch pixel resolution, the UAS can cover 541 acres per charge; at a 4-inch resolution it can cover over 1200 acres per charge.

Application of UASs in Pavement Monitoring

Distress in pavement surfaces usually manifests in the form of surface cracking, roughness, rutting, permanent deformation, or bumps and is caused by its interaction with vehicular traffic, thereby affecting the functional and structural performance of the pavement (Adu-Gyamfi et al., 2014).



Fig. 1 a) Aibotix X6 rotary-type UAS; b) UX 5 fixed wing UAS (Leica Geosystems)

Currently, various departments of transportation (DOTs) conceptualize existing road conditions based on their own pavement distress databases, wherein data is gathered either via physical inspection by engineers/expert technicians or by using road vehicles mounted with optical sensors.

Such traditional methods are expensive, collect only localized data, have poor repeatability due to surveys conducted by different operators, can endanger the safety of personnel involved due to traffic accidents, and may cause delays in processing data (Oh, 1998; Mustaffar et al., 2008). This makes it difficult for the decision-making managers to achieve cost-effective road maintenance plans while staying within budgetary constraints (Shamsabadi et al., 2014). In addition, there is a growing need to perform continuous health monitoring of complete road networks rather than doing repairs for localized patches. Incorporation of accurate data regarding present pavement conditions, along with models predicting the rate of deterioration within the management frameworks, identifies and prioritizes future maintenance and improves the management plan for maintenance, rehabilitation, and/or reconstruction (Adu-Gyamfi et al., 2014). AASHTO defines “physical failure (deterioration)” as one of the major types of risks, reinforcing the importance of continuing health monitoring (AASHTO 2011).

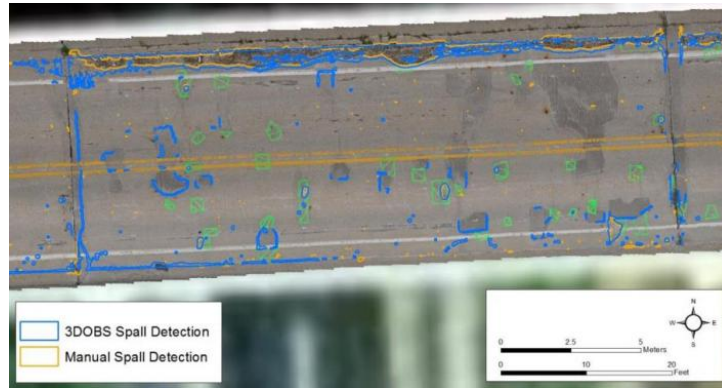


Fig. 2. Manual and automated detection of pavement distress (spalls) at Willow Road Bridge near Milan, MI (Brooks et al., 2015; MTRI 2016).

Fig. 2 depicts a reconstructed orthophoto that was created from a series of photos with a Nikon D5000 camera at Willow Road Bridge near Milan, Michigan. It shows pavement distress, in the form of spalls, detected both manually and through image analysis (Brooks et al., 2015; MTRI 2016). Recent developments in digital photogrammetric technology have provided a low-cost and nearly real-time geometrical imaging technique that can be performed without physically invading the pavement. Mustaffar et al. (2008) used a digital photogrammetric system, combined with an automated pavement imaging program (APIP), to measure pavement distress, such as longitudinal, transverse, and alligator cracking. Accuracy was approximately 90 percent that of traditional methods.

Fig. 3a shows the rotary-type UAV (Berger Tazer 800 helicopter), with a camera attached, employed by Michigan Technological University for aerial surveys of pavements and bridges. Fig. 3b shows the captured high resolution image from a Tazer 800 UAV that was fitted with a Nikon D800 DSLR camera (Brooks et al. 2015).

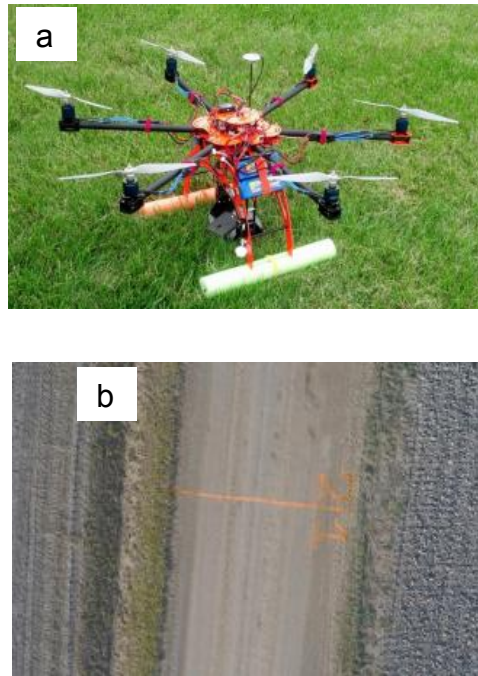


Fig. 3 a) Bergen Tager 800 helicopter UAV (rotary wing) with digital camera; b) High-resolution image collected from Tager 800 UAV camera (Brooks et al. 2015)

Application of UASs in Bridge Monitoring

Recently, the DJI Phantom 2 UAV (quadcopter), which can fly in relatively challenging areas such as beneath bridges and inside confined spaces, was employed for aerial surveys during a research program conducted jointly by the Michigan Tech Research Institute and Michigan Tech Transportation Institute (Brooks et al., 2015). The camera, which has the capacity to take pictures and record video to micro SD cards with a real-time video link of up to 900 feet, was mounted on the DJI Phantom Vision 2 UAS. It was used to create photographic inventories of study sites, such as bridges with hard-to-reach areas, and to look for damage on the inside of a pump station. Fig. 4 shows the same DJI Phantom Vision 2 UAS, with a small (GoPro) camera mounted on its top to shoot photos of the underside of bridges.



Fig. 4. DJI Phantom Vision 2 quadcopter UAS performing under-bridge inspection (Brooks et al., 2015; www.mtri.org).

Photogrammetric output, such as digital maps and orthophotos, can be successfully obtained from small-format cameras. Once analyzed, the data can be used to compare and assess any changes in the infrastructure.

Ground Improvement with Chemical Stabilization

Chemical Stabilizers

Lime reduces the swelling potential, liquid limit, plasticity index, and maximum dry density of the soil and increases its optimum water content, shrinkage limit, and strength (Croft, 1967). It improves the workability and compaction of subgrade soils (Jung et al., 2008). When clay soil is treated with lime and reacts in the presence of water, new compounds are formed through the processes of cation exchange, flocculation, carbonation, and pozzolanic reaction (Al-Rawas et al., 2005). The length of time required for these processes to be completed can vary, depending on the type of clay being treated. Therefore, lime-treated soil is allowed one to four days for mellowing, which helps to establish a consistent or homogeneous mixture (Al-Rawas et al., 2005; Puppala et al., 2006; Chittoori et al., 2013).

Lime stabilization is a widely-used means of chemically transforming unstable soils into structurally sound foundations. Lime stabilization enhances engineering properties in soils by improving strength; improving resistance to fracture, fatigue, and permanent deformation; improving resilient properties; reducing swelling; and enhancing resistance to the damaging effects of moisture. The most substantial improvements in these properties are seen in moderately-to-highly plastic clays (Little, 1999; Puppala et al., 2006, 2013). When lime is combined with water and the soluble silica and alumina present in clay, a chemical reaction occurs, resulting in the formation of new compounds. During this reaction, the primary function of lime is to alter the particle structure and increase resistance to shrink-swell behavior and moisture susceptibility.

A secondary result is an increase in strength caused by the binding of particles through chemical gels, including formed tobermorite gels (Al-Rawas et al., 2005). Tobermorite gels are typically formed due to hydration of calcium silicates and result in the hardening of treated soils. Since alteration of particle structure occurs slowly, depending upon the type of clay present, a mellowing period of one to four days can produce a homogeneous, friable mixture. Many researchers successfully use lime as a stabilizer to modify soils and enhance the soil's properties.

Soils that have a plasticity index (PI) value higher than 30 are not typically used for stabilization or mixed with cement. To bypass this issue, lime can be added prior to adding the cement, which will keep the soil more pliable (Hicks, 2002). Many researchers have successfully treated subsoils with a mixture of lime and cement. Sirivitmaitrie et al. (2008) studied a combined lime-cement stabilization method performed on several soils from Arlington, Texas, USA. Laboratory tests, including Atterberg limits, unconfined compressive strength (UCS) tests, resilient modulus (MR), vertical swell, and linear shrinkage bar tests were conducted on untreated soils, lime-treated soils (lime making up 12% by dry weight of soil), and lime-and-cement treated soils (6% lime and 6% cement). The resilient moduli test results showed that the moduli were significantly higher for lime-cement treated soils. After laboratory studies, several pavement test sections were built on lime-cement treated soils, and the performance data indicated that these treatments provided effective stabilization of soils in Arlington, Texas. Based upon this study, Sirivitmaitrie et al. (2008) recommended that the stabilizer dosage be reduced from a total of 12% to 8%, which may provide stable and uniform support to pavements.

Fly ash is one of four coal combustion products (CCPs) that are produced as a byproduct of burning coal for generating electricity in the United States. The remaining three types are bottom ash, boiler slag, and flue gas desulfurization byproduct material (i.e., gypsum). Fly ash makes up 58% of CCPs; of this 58%, only 32% is reused in construction. Its primary construction application is its use as part of the base material in highways. Another benefit of its use in civil applications is that less fly ash will be placed in a landfill, thereby reducing landfill costs and mitigating environmental impacts (Arora and Aydilek, 2005).

Coal burning power plants do not produce the same types of fly ash since each plant is operated differently and may use a different type of coal. Two major groups of fly ash are produced: Class C and Class F. Burning lignite and subbituminous coal produces Class C fly ash, whereas burning anthracite, also known as bituminous coal, produces Class F fly ash (Çokça, 2001). Although there can be multiple variations of the chemical additive, fly ash particles generally consist of hollow spheres of silicon, aluminum, iron oxides, and carbon, all of which make both classes of fly ash pozzolans-siliceous or siliceous and aluminous materials. Class F fly ash is not used as often as Class C because it is not a self-cementing material and requires an activator, either lime or cement, to form pozzolanic stabilized mixtures (PSMs) (Arora and Aydilek, 2005).

A combination of lime and fly ash is effective for stabilizing silty and sandy soils because it drastically increases the stiffness of the final product. Bergeson and Barnes (1998) used Class C fly ash with lime to develop guidelines for determining the structural layer coefficient for the base layer of flexible pavement, and showed that the required base-layer thickness decreases with the addition of both additives. Although lime, cement, and fly ash are commonly-used stabilizers, there are many other options in the market, such as cement bypass dust (CBPD), also known as cement kiln dust (CKD); lime kiln dust (LKD); blast furnace slag; and others (Al-Rawas et al., 2002). These are supplementary and secondary stabilizers that do not work well alone. They require a primary stabilizing agent, such as lime or cement additives, to initiate the stabilization reactions (Chittoori et al., 2013; Puppala, 2016).

Lightweight Materials in Infrastructure

Various lightweight materials have been used in earthworks construction, including EPS (expanded polystyrene) geofoam, foamed Portland cement concrete, wood fibers, shredded tires, expanded shale and clays, boiler slag, air-cooled blast furnace slag, fly ash, and expanded blast furnace slag. The following section discusses the use of EPS geofoam as a partial substitute material in road embankments.

Project Description

The bump at the end of a bridge is a pervasive problem that is common to most bridge infrastructures. It is frequently encountered in Texas and many other states, and transportation agencies spend millions of dollars annually to repair them. The major cause of the problem is the settlement of the backfill materials and foundation soils, as well as the erosion of the backfill, and is due to the settlement of the approach slabs with reference to the bridge deck level. Several technologies to solve this problem have been tried by various organizations; however, the settlement issue of the approach slabs on high embankments seems to persist.

A site in Johnson County, Texas, USA experiences huge settlements and was the focus of a research project launched at the University of Texas at Arlington. It is located on US 67 over SH 174 in Cleburne, Texas. The bridge is 12.2 m (40 ft.) high, and in the 16 years since its

construction, the approach slab has experienced more than 16 in. of settlement, as shown in Fig. 5. One of the primary causes of the settlement is the self-weight of the 40-ft high embankment fill material which undergoes self-consolidation, inducing large stresses and settlement to the underlying foundation subgrade. To mitigate the settlement, several treatment methods were applied, including hot mix overlays, grout injections, soil nailing, and others; however, they were not effective.

Laboratory studies were conducted on the basic properties of the soil, including compressibility characteristics and shear strength, and on the properties of the EPS 22 geofoam. Field monitoring studies were also conducted at regular time intervals to study the performance of the EPS geofoam under live traffic. Modeling studies were conducted, using the PLAXIS program, to predict the long-term performance of the test section.



Fig. 5 Bridge approach slab settlement in Johnson County, Texas, USA

The Texas Department of Transportation (TxDOT) considered several lightweight fill materials to reduce the self-weight of the soil, and selected EPS geofoam as an embankment fill material. The lightweight and compact EPS geofoam material has specific advantages, such as ease of construction, lighter weight (at least 20 to 30 times lighter than other lightweight fill alternatives), ability to reduce the lateral stresses on retaining walls, limited labor costs, and an expedited construction schedule, which reduces the overall cost of the structures (Archeewa, 2010).

The embankment was reconstructed, replacing the top of the existing fill soil with lightweight EPS 22 geofoam blocks to reduce the loads imposed on the underlying subgrade and to reduce the magnitude of settlement due to the consolidation phenomenon. Because of the huge settlements, the quality assurance studies of the performance of the geofoam approach slab was the key aspect of this study. The following sections discuss the site location and quality assurance studies conducted for this project. The research is ongoing to achieve the final objective, which is to develop design and construction guidelines, for future use, on other geofoam-related construction.

Site Description

The test site was located at the intersection of US 67 and State Highway 174 in Johnson County, Texas USA, as illustrated in Fig. 6. The bridge was designed for two-lane traffic, and both ends

of the bridge were placed on abutments supported by drilled shaft foundations. Approach embankments were built adjacent to the bridge abutments to support the interfacing bridge approach slabs and roadways. The embankment fill soils were classified as clayey sand (SC), and the foundation soils were classified as clays of low plasticity (CL), as per the USCS classification.



Fig. 6 Test site location

Construction with EPS Geofoam

The rehabilitation of the test site began in January 2012. The test site was constructed with EPS 22 geofoam, which has unit weight of 24.35 kg/m^3 (1.52 pcf) and unconfined compressive strength of 152 kPa (3174 psf). The embankment soils were first excavated to a depth of about 2.74 to 3.04 m (8 to 10 ft.).

A sand layer was put in place to provide a proper leveling base before the installation of the EPS geofoam. The geofoam blocks were then placed on top of the sand layer to a height of 1.83 m (6 ft.) and were connected, using a barbed plate, and encapsulated in a geotextile membrane, which protected the geofoam blocks from the infiltration of any fluids and termite infestations. Fig. 7 illustrates the construction process of the EPS geofoam. Different sizes of the geofoam blocks were used in this construction to fill all the narrow spaces. A pavement structure of 0.61 m (2 ft.) was placed on top of the geofoam blocks, using a flex base and hot mix asphalt concrete (HMAC) pavement surface.



Fig. 7 Construction of EPS Geofoam

Instrumentation Details

The test site was instrumented to monitor the settlement and pressure that was exerted on the structure. Horizontal inclinometers, which measured the displacement of the subsurface layers in a direction perpendicular to the axis of a flexible plastic casing, were used to monitor the settlement. Four small trenches were excavated in the top geofoam blocks in accordance with the size of the inclinometer casing, as shown in Fig. 8.

Long PVC casing pipes of about 7.9 m (24 ft.) were installed in the trenches, and the extended ends of the casings were fastened with cast-in-place concrete bases. Four earth pressure cells, made of two circular stainless steel plates welded together to form a sealed cavity, were installed in the embankment to monitor the pressures exerted on the structure. The cavity was filled with a non-compressible fluid, and a pressure transducer was connected to the cell. Fig. 9 depicts the installation of the pressure cells in the embankment. A Quattro Logger, a compact data logger, was used to monitor the four installed pressure cells. The logger was automated to record the pressures at 15-minute intervals. The recorded data was retrieved after every site visit.



Fig. 8 Horizontal inclinometers installation

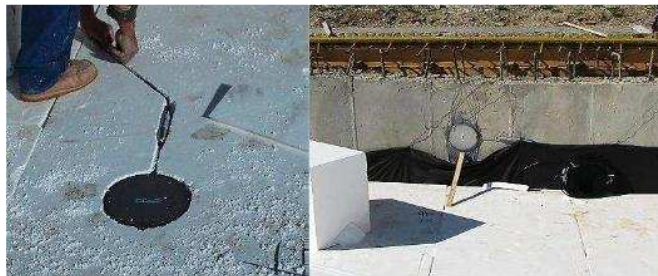


Fig. 9 Pressure cell installation

Results and Analysis

The horizontal inclinometer and pressure cell readings were taken monthly to evaluate the performance of the geofoam block structure. Fig. 10 presents the plot of the cumulative settlement of the embankment along the inclinometer casing at one station.

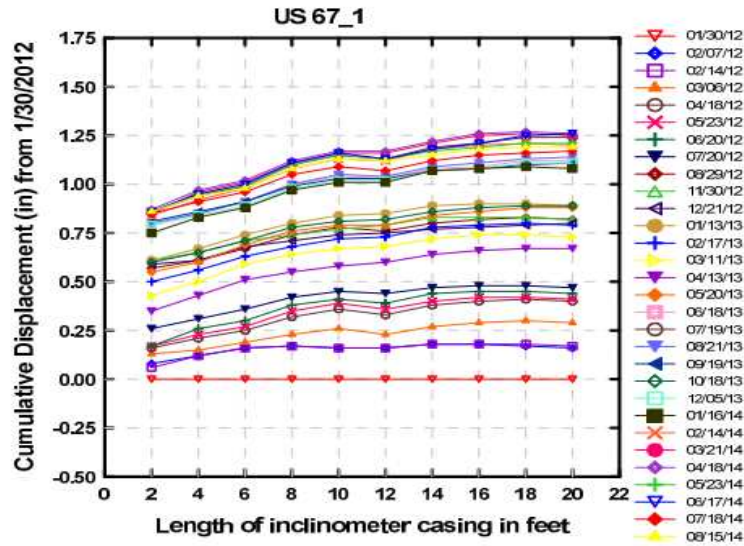


Fig. 10 Horizontal Inclinometer readings

The data was collected in January 2012, immediately after the installation. From the plots, it can be observed that the maximum displacement was less than 33 mm (1.5 in.). This means that the geofoam blocks can sustain the traffic load effectively and can mitigate the settlements (Ruttanaporamakul 2014), thus assuring the quality of the geofoam blocks' performance in the bridge approach slabs.

The data recorded from the pressure cells depicted an average vertical pressure of 33.8 kPa (4.9 psi) and 12.4 kPa (1.8 psi) from pressure cells 1 and 2. The pressure cells, that were installed to measure the lateral pressures, provided negative values due to the loss of contact of the pressure cell to the EPS geofoam layer and abutment walls.

Summary and Conclusions

Based on the studies discussed in the first section of this paper, a combination of the UAV system and photogrammetry seems to be a promising technology. However, its performance in the transportation arena and in the geotechnical environment has been minimally explored, and more research is needed.

The second case study evaluated the performance of the geofoam blocks used as fill material in the embankment to arrest settlement of the approach slab. The use of instrumentation, such as horizontal inclinometers and pressure cells, provided the real field settlements and pressures that were occurring in the bridge approach slabs.

Additional studies using remote sensing equipment, such as the terrestrial Lidar and UAVs mounted with cameras, are ongoing at the University of Texas at Arlington. In the future, this data will be compared with that of the conventional instruments that was presented in this study.

ACKNOWLEDGEMENTS

The author would like to acknowledge Mr. David Marshall, Ms Shelly Hattan, and Mr. Richard S. Williammee for their valuable assistance and cooperation throughout the research.

REFERENCES

- Adu-Gyamfi, Y.O., Teenaah, T., Attoh-Okine, N. O., and Kambhamettu, C. (2014). "Functional evaluation of pavement condition using a complete vision system." *J. Transp. Eng.*, vol. 140 (9), ASCE, pp. 1-10.
- Ahmad, A. (2006) "Digital photogrammetry: An experience of processing aerial photograph of UTM acquired using digital camera." In *AsiaGIS*, 3-5 March; UTM Skudai, Johor, Malaysia, pp. 1-11.
- Al-Rawas, A. A., Hago, A. W., and Al-Sarmi, H. (2005). "Effect of lime, cement and Sarooj (artificial pozzolan) on the swelling potential of an expansive soil from Oman." *Build. Environ.*, 40(5), 681-687.
- American Association of Highway and Transportation Officials (AASHTO) (2011). *AASHTO transportation asset management guide: a focus on implementation*. Washington, D.C.: AASHTO, 2011.
- Archeewa, E. (2010). "Comprehensive studies on deep soil mixing and lightweight aggregates application to mitigate approach slab settlements." Dissertation submitted in partial fulfillment of the requirements for the degree of the Doctor of Philosophy, the University of Texas at Arlington, Arlington, Texas.
- Arora, S., and Aydilek, A. (2005). "Fly-ash amended soils as highway base materials." *J. Mater. Civ. Eng.*, ASCE, 17(6), pp. 640-649.
- Bergeson, K. L., and Barnes, A. G. (1998). "Iowa thickness design for low volume roads using reclaimed hydrated class C fly ash bases." USUERI-Ames 98401, Iowa State University, Ames, Iowa, pp. 253-258.
- Brooks, C. N., Oommen, T., Havens, T. C., Ahlborn, T. M., Zhang, K., Mukherjee, A., and Dobson, R. (2015). "Implementation of unmanned aerial vehicles (UAVs) for assessment of transportation infrastructure – Phase II." Prepared by Michigan Technological University for MDOT, 68 pgs., www.mtri.org.
- Brooks, C., Dobson, R. J., Banach, D. M., Dean, D., Oommen, T., Wolf, R. E., Havens, T. C., Ahlborn, T. M. and Hart, B. (2015). MDOT: "Evaluating the use of unmanned aerial vehicles for transportation purposes." Michigan Tech Research Institute and Michigan Tech Transportation Institute, Final report No. RC-1616, Revised version April 7, 2015, www.mtri.org.
- Cesetti A., Frontoni E., Mancini A., Ascani A., Zingaretti P. and Longhi S. (2011). "A visual global positioning system for unmanned aerial vehicles used in photogrammetric applications." *Journal of Intel Robot systems*, vol. 61, pp. 157-168.
- Chen F. H. (1988). *Foundations on expansive soils*. 2nd ed. New York: Elsevier Science Publications.
- Chittoori, B. C. S., Puppala, A. J., Wejrengsikul, T., and Hoyos, L. R. (2013). "Experimental studies on stabilized clays at various leaching cycles." *ASCE, J. Geotech. Geoenviron. Eng.*, 139(10), 1665-1675.
- Cokca, E. (2001). "Use of class C fly ashes for the stabilization of an expansive soil." *J. Geotech. Geoenviron. Eng.*, 127(7), pp. 268-273.
- Colomina I., and Molina P. (2014). "Unmanned aerial systems for photogrammetry and remote sensing: a review." *ISPRS Journal of Photogrammetry and Remote Sensing*, vol. 92, pp.79-97.

- Croft, J. B. (1967). "The influence of mineralogical composition on cement stabilization." *Geotechnique*, 17: 119-135.
- De Bel R., Correia, A. G., Verbrugge, J. C. (2009). "Contribution of loamy soil treatment to improve embankments performance." *Geotech. Spec. Publ.*, 189, pp. 186-191.
- Hicks, R. G. (2002). *Stabilization design guide*. FHWA_AK_RD_01-6B, Oregon State University., Corvallis, Oregon, TRB: 2002.
- Jung, C., Bobet, A., Siddiki, N. Z., and Kim, D. (2008). "Long-term performance of chemically modified subgrade soils in Indiana." *Transp. Res. Rec.*, 2059, 63-71.
- Little, D. N. (1999). "Evaluation of structural properties of lime stabilized soils and aggregates: Vol. 1, Summary of Findings." National Lime Association Publication.
- Mills, J.P. and Newton, I. (1996). "Aerial photography for survey purposes with a high resolution small format digital camera." *Photogrammetric Record*, vol. 15(88), pp. 575-587.
- Mustaffar, M., Ling, T. C., and Puan, O. C. (2008). "Automated pavement imaging program (APIP) for pavement cracks classification and quantification – A photogrammetric approach." *The International Archives of the photogrammetry. Remote sensing and spatial information science*, 37(B4): pp. 367-372.
- Nelson J. D., and Miller J. D. (1992). *Expansive soils: Problems and practice in foundation and practice in pavement engineering*. Wiley, New York: Colorado State University.
- Oh, H. (1998). "Image processing technique in automated pavement evaluation system." University of Connecticut: Ph.D. Dissertation.
- Oscar, E. S., Ellen, M. R., and Buckely, S. M. (2013). "Deformation of a rapidly moving landslide from high-resolution optical satellite imagery." *Geo-Congress 2013, ASCE, San Diego, CA, March 3-7, 2013, GSP 231*, pp. 269-278.
- Pedarla, A., Chittoori, B. C. S., Puppala, A. J. (2011). "Influence of minerology and plasticity index on the stabilization effectiveness of expansive clays." *J. Transp. Res. Board, Nat. Acad. Sci., Transp. Res. Board*, 2212: 91-99.
- Pereira, E., Bencatel, R., Correia, J., Felix, L., Goncalves, G., Morgado, J., and Sousa, J. (2009). "Unmanned air vehicles for coastal environmental research." *Journal of Coastal Research, SI 56 (Proceedings of the 10th International Coastal Symposium)*, 1557-1561, Lisbon, Portugal, ISSN 0749-0258.
- Puppala, A. J. (2016). "Advances in ground modification with chemical additives: From theory to practice." *Transportation Geotechnics*, 9, 123-138.
- Puppala, A. J., Chittoori, B. C. S., Talluri, N., Le, M., Bheemasetti, T., and Thomey, J. (2013). "Stabilizer selection for arresting surficial slope failures: A sustainability perspective." *ASCE GeoCongress, San Diego, California*, pp. 1465-1474.
- Puppala, A. J., Kadam, R., Madhyannapu, R., and Hoyos, L. R. (2006). "Small strain shear moduli of chemically stabilized sulphate-bearing cohesive soils." *J. Geotech. Geoenviron. Eng.*, 1(32), 322-336.
- Rathje, E. M., Woo, K., and Crawford, M. (2006). "Spaceborne and airborne remote sensing for geotechnical applications." *GeoCongress 2006: Geotechnical Engineering in the Information Technology Age, Atlanta, Georgia, US, February 26-March 1, 2006*, pp.1-19.
- Ruttanaporamakul, P. (2014). *Evaluation of lightweight geofoam for mitigating bridge approach slab settlements*. Doctoral dissertation, The University of Texas at Arlington, Texas, USA.

- Room, M.H.M., and Ahmad, A. (2014). "Mapping of river using close range photogrammetry technique and unmanned aerial vehicle system." 8th International Symposium of the Digital Earth, Earth and Environmental Science, vol. 18, pp. 1-6.
- Shamsabadi, S. S., Wang, M., and Birken, R. (2014). "PAVEMON: A GIS-based data management system for pavement monitoring based on large amounts of near-surface geophysical sensor data." 27th Symposium on the Application of geophysics to engineering and environmental problems 2014, pp. 130-133, Red Hook, NY, Curran.
- Siebert, S., and Teizer, J. (2014). "Mobile 3D mapping for surveying earthwork projects using an unmanned aerial vehicle system." Automation in Construction, vol. 41, pp. 1-14.
- Sirivitmaitrie, C., Puppala, A. J., Saride, S., and Hoyos, L. R. (2008). "Combined lime and cement treatment of expansive soils." ASCE, Geotechnical Special Publication, 178, Geo-Congress, New Orleans, Louisiana, pp. 646-653.
- Tahar, K. N., and Ahmad, A. (2012). "A simulation study on the capabilities of rotor wing unmanned aerial vehicle in aerial terrain mapping." International Journal of Physical Sciences, 7(8), pp. 1300-1306.
- Tripolitsiotis, A., Chrysanthos, S., Eirini, P., Zacharias, A., Stelios, M., and Panagiotis, P. (2014). "Complementing geotechnical slope stability and land movement analysis using satellite DinSAR." Central European Journal of Geosciences, Ist International Conference on Remote Sensing and Geoinformation of Environment, vol. 6, No. 1, pp. 56-66, March 2014.
- Tronin, A. A. (2010). "Satellite remote sensing in seismology – A review." Remote Sensing, vol. 2, pp. 124-150, doi: 10.3390/rs2010124.
- Udin, W. S. and Ahmad, A. (2014). "Assessment of Photogrammetric Mapping Accuracy Based on Variation Flying Altitude Using Unmanned Aerial Vehicle." 8th International Symposium of the Digital Earth, Earth and Environmental Science, vol. 18, pp. 1-7.
- Yi, Y., Liu, S., and Puppala, A. J. (2016) "Laboratory modeling of T-shaped soil-cement column for soft ground treatment under embankment." Geotechnique, 66(1), 85-89.